

A BACKWARD PROBLEM FOR THE TIME-FRACTIONAL PSEUDO-PARABOLIC EQUATION WITH A VARIABLE COEFFICIENT

ARSHYN ALTYBAY

ABSTRACT. This work addresses an inverse reconstruction task for a time-fractional pseudo-parabolic model with a temporally varying coefficient. By imposing Dirichlet boundary conditions, we aim to recover the unknown initial state from observations collected at the final time.

From a theoretical perspective, we derive existence and uniqueness results by proving that, under suitable hypotheses, the problem admits a unique solution. Computationally, we introduce a finite-difference discretisation based on a time-stepping strategy and provide a detailed stability and convergence analysis. Leveraging the resulting forward solver, we then formulate an initial-data identification procedure using Tikhonov regularisation. The proposed approach is validated with numerical simulations, and its resilience is assessed via experiments that incorporate perturbations in the final-time measurements.

1. INTRODUCTION

Pseudo-parabolic equations (Sobolev-type equations) are a mathematical model for a wide class of important physical and mechanical applications, such as filtration processes in porous media [1], population aggregation dynamics [2], nonlinear long-wave propagation [3, 4], second-order unsteady fluid flows [5], fluid transport in fractured rocks [6], and non-Newtonian fluid motion [7, 8]. The inverse problems for a linear, semilinear and nonlinear pseudoparabolic equation, both by itself and with variable coefficients, have been extensively investigated; a representative selection of related works can be found in [9]–[22].

To the best of our knowledge, only a limited number of studies have addressed backward problems for the time-fractional pseudo-parabolic equation, particularly with rigorous numerical analysis and the presence of noisy data.

In this work, we study a backward problem for a time-fractional pseudo-parabolic equation

$$\partial_t^\alpha u(x, t) - u_{xx}(x, t) - \mu(t) u_{xxt}(x, t) = f(x, t), \quad (x, t) \in (0, l) \times (0, T), \quad (1.1)$$

subject to the Dirichlet boundary conditions

$$u(0, t) = u(l, t) = 0, \quad t \in [0, T], \quad (1.2)$$

and the final-time measurement

$$u(x, T) = \psi(x), \quad x \in [0, l]. \quad (1.3)$$

Here, $u(x, t)$ denotes the temperature, $f(x, t)$ is a given source term, $\mu(t)$ is a pseudo-parabolic coefficient, and ψ is the measured final-time state. The operator

Key words and phrases. backwards-in-time problem, time-fractional pseudo-parabolic equation, Volterra integral equations, Tikhonov regularisation, numerical analysis.

∂_t^α denotes the Caputo fractional derivative of order $\alpha \in (0, 1)$. Following [23], it is given by

$$\partial_t^\alpha u(x, t) = \frac{1}{\Gamma(1-\alpha)} \int_0^t (t-s)^{-\alpha} \partial_s u(x, s) ds,$$

with $\Gamma(\cdot)$ standing for the Gamma function.

The backwards-in-time problem consists of reconstructing the initial state

$$u_0(x) := u(x, 0), \quad x \in [0, l], \quad (1.4)$$

and, consequently, the whole trajectory u on $[0, T]$ from the data (f, ψ) .

The equation (1.1) models a time-fractional pseudo-parabolic diffusion process with memory and relaxation effects, describing anomalous transport phenomena influenced by time-dependent material properties and external forcing in the space-time domain $(0, l) \times (0, T)$. In engineering applications, backwards-in-time problems are essential because they focus on reconstructing past physical states using data observed at a later time.

A pioneering contribution to the well-posedness analysis of the backward-in-time problem for the time-fractional diffusion equation is given in [24]. Further developments for backward problems in fractional diffusion-wave models include theoretical and numerical studies in bounded domains [25], as well as iterative regularisation approaches (e.g., Landweber-type methods) for identifying unknown initial data in time-space fractional settings [26]. General well-posedness frameworks for backwards-in-time problems for time-fractional diffusion and diffusion-wave equations were also established in [27, 28]. In addition, simultaneous recovery of multiple initial values for time-fractional diffusion-wave equations was investigated in [30].

For fractional pseudo-parabolic equations, backward problems and related stability issues have been analysed in [29, 31]. Regularisation methods for reconstructing the initial value in time-fractional pseudo-parabolic models were developed in [33], and robustness under random noise was further studied in [34]. Related inverse initial data problems for time-fractional pseudo-hyperbolic equations were considered in [35].

Despite recent progress, backwards-in-time analysis for time-fractional pseudo-hyperbolic equations remains underexplored, particularly in terms of well-posedness theory, numerical reconstruction, and noisy data treatment. To address this deficiency, we undertake a comprehensive theoretical and numerical investigation of the problem.

Our contributions are threefold. From a theoretical perspective, we establish the existence and uniqueness of the backwards-in-time problem for a time-fractional pseudo-parabolic equation with a time-dependent coefficient. From a numerical perspective, we design a stable finite-difference discretisation and prove corresponding stability and convergence estimates. From a computational perspective, we develop a noise-robust reconstruction algorithm based on the proposed finite difference scheme combined with Tikhonov regularisation.

The remainder of the manuscript is structured as follows: Section 2 establishes the existence and uniqueness of the backward problem. Section 3 develops and analyses a stable numerical scheme for the direct model. Section 4 presents the reconstruction procedure for identifying the unknown initial state from finite-time measurements. Numerical validations, including tests with noisy data, are given in Section 5.

2. EXISTENCE AND UNIQUENESS OF THE PROBLEM

In this section, we establish the existence and uniqueness of a solution to the backwards-in-time problem for the time fractional pseudo-parabolic equation (1.1) subject to the Dirichlet boundary conditions (1.2) and the final-time measurement (1.3).

2.1. Definition and assumptions.

Definition 2.1. A pair (u, u_0) is called a classical solution of (1.1)–(1.3) if

$$u \in C([0, T]; C([0, l])) \cap C^1((0, T); C^2([0, l])), \quad u_0 \in C([0, l]),$$

and, in addition,

$$\partial_t^\alpha u \in C((0, T) \times [0, l]),$$

where the Caputo derivative is defined by

$$\partial_t^\alpha u(x, t) = \frac{1}{\Gamma(1-\alpha)} \int_0^t (t-s)^{-\alpha} \partial_s u(x, s) ds, \quad (x, t) \in [0, l] \times (0, T).$$

Moreover, $u(\cdot, 0) = u_0$ on $[0, l]$, $u(0, t) = u(l, t) = 0$ for $t \in [0, T]$, $u(\cdot, T) = \psi$ on $[0, l]$, and (1.1) holds pointwise on $(0, l) \times (0, T)$.

Assumptions. Throughout this section, we assume:

F1 $\alpha \in (0, 1)$, $\mu \in C([0, T])$, and there exists $\mu_0 > 0$ such that $\mu(t) \geq \mu_0$ for all $t \in [0, T]$.

F2 $\psi \in H^3(0, l)$ and

$$\psi(0) = \psi(l) = 0, \quad \psi''(0) = \psi''(l) = 0.$$

F3 $f \in L^2(0, T; H^3(0, l))$ and for a.e. $t \in (0, T)$,

$$f(0, t) = f(l, t) = 0, \quad f_{xx}(0, t) = f_{xx}(l, t) = 0.$$

For uniform-in-time estimates of the time-derivative series we shall also use:

F4 For every $\delta \in (0, T)$, $f \in L^\infty(\delta, T; H^3(0, l))$.

2.2. Existence and uniqueness.

Theorem 2.2 (Existence, uniqueness, and explicit reconstruction). *Let **F1–F4** hold. Then the inverse problem (1.1)–(1.3) admits a unique classical solution (u, u_0) in the sense of Definition 2.1. Moreover, (u, u_0) is given by*

$$u(x, t) = \sum_{k=1}^{\infty} \left[\frac{\mathcal{A}_k(t)}{\mathcal{A}_k(T)} \psi_k + \mathcal{B}_k(t) - \frac{\mathcal{A}_k(t)}{\mathcal{A}_k(T)} \mathcal{B}_k(T) \right] e_k(x), \quad (x, t) \in [0, l] \times [0, T], \quad (2.1)$$

$$u_0(x) = \sum_{k=1}^{\infty} \left[\frac{\psi_k - \mathcal{B}_k(T)}{\mathcal{A}_k(T)} \right] e_k(x), \quad x \in [0, l], \quad (2.2)$$

where

$$e_k(x) = \sin\left(\frac{k\pi}{l}x\right), \quad \lambda_k = \left(\frac{k\pi}{l}\right)^2, \quad k = 1, 2, \dots,$$

ψ_k and f_k are defined in (2.4), and $\mathcal{A}_k, \mathcal{B}_k$ are defined by (2.7) below. In particular, Lemma 2.3 yields $\mathcal{A}_k(T) > 0$, so the coefficients in (2.1)–(2.2) are well-defined.

Furthermore:

- (i) The series (2.1) converges uniformly on $[0, l] \times [0, T]$ and the series for u_{xx} converges uniformly on $[0, l] \times [0, T]$.
- (ii) For every $\delta \in (0, T)$ the series for u_t , u_{xxt} and $\partial_t^\alpha u$ converge uniformly on $[0, l] \times [\delta, T]$.

Proof. Formal Solution. Let $\{e_k\}_{k \geq 1}$ be the sine eigenfunctions of $-\partial_{xx}$ on $(0, l)$:

$$e_k(x) = \sin\left(\frac{k\pi}{l}x\right), \quad -e_k'' = \lambda_k e_k, \quad \lambda_k = \left(\frac{k\pi}{l}\right)^2.$$

Then $\{e_k\}_{k \geq 1}$ is an orthogonal basis of $L^2(0, l)$ with

$$\int_0^l e_k(x)e_j(x) dx = \frac{l}{2}\delta_{kj}.$$

For $v \in L^2(0, l)$ define its sine and cosine Fourier coefficients

$$v_k := \frac{2}{l} \int_0^l v(x) \sin\left(\frac{k\pi}{l}x\right) dx, \quad v_k^c := \frac{2}{l} \int_0^l v(x) \cos\left(\frac{k\pi}{l}x\right) dx.$$

Then Parseval's identity and Bessel's inequalities read

$$\|v\|_{L^2(0, l)}^2 = \frac{l}{2} \sum_{k=1}^{\infty} |v_k|^2, \quad \sum_{k=1}^{\infty} |v_k|^2 \leq \frac{2}{l} \|v\|_{L^2(0, l)}^2, \quad \sum_{k=1}^{\infty} |v_k^c|^2 \leq \frac{2}{l} \|v\|_{L^2(0, l)}^2. \quad (2.3)$$

Assume that f and ψ have sine-series expansions

$$f(x, t) = \sum_{k=1}^{\infty} f_k(t) e_k(x), \quad \psi(x) = \sum_{k=1}^{\infty} \psi_k e_k(x),$$

where $f_k(t)$ and ψ_k are the sine coefficients of f and ψ defined by

$$f_k(t) = \frac{2}{l} \int_0^l f(x, t) \sin\left(\frac{k\pi}{l}x\right) dx, \quad \psi_k = \frac{2}{l} \int_0^l \psi(x) \sin\left(\frac{k\pi}{l}x\right) dx, \quad (2.4)$$

$k = 1, 2, \dots$, respectively.

We seek solution of (1.1)-(1.3) in the sine-series expansion form: Expanding u in the sine basis,

$$u(x, t) = \sum_{k=1}^{\infty} u_k(t) e_k(x), \quad e_k(x) = \sin\left(\frac{k\pi}{l}x\right),$$

and using $u_{xx} = -\sum_{k \geq 1} \lambda_k u_k e_k$ and $u_{xxt} = -\sum_{k \geq 1} \lambda_k u_k' e_k$, we obtain for each $k \geq 1$ the mode equation

$$\partial_t^\alpha u_k(t) + \mu(t) \lambda_k u_k'(t) + \lambda_k u_k(t) = f_k(t), \quad 0 < t < T, \quad u_k(T) = \psi_k. \quad (2.5)$$

Let $y_k(t) := u_k'(t)$ and $u_{0,k} := u_k(0)$. Then

$$u_k(t) = u_{0,k} + \int_0^t y_k(s) ds, \quad \partial_t^\alpha u_k(t) = \frac{1}{\Gamma(1-\alpha)} \int_0^t (t-s)^{-\alpha} y_k(s) ds.$$

Substituting into (2.5) yields the Volterra equation

$$y_k(t) + \int_0^t H_k(t, s) y_k(s) ds = \frac{f_k(t) - \lambda_k u_{0,k}}{\mu(t) \lambda_k}, \quad 0 < t < T,$$

where

$$H_k(t, s) = \frac{1}{\mu(t)} + \frac{1}{\mu(t) \lambda_k \Gamma(1-\alpha)} (t-s)^{-\alpha}, \quad 0 \leq s < t \leq T.$$

Let R_k be the corresponding resolvent kernel (given by the Neumann series). Then

$$y_k(t) = g_k(t) + \int_0^t R_k(t, s)g_k(s) ds, \quad g_k(t) := \frac{f_k(t) - \lambda_k u_{0,k}}{\mu(t)\lambda_k}.$$

Integrating in time and using $u_k(t) = u_{0,k} + \int_0^t y_k(\tau) d\tau$ yields

$$u_k(t) = u_{0,k} \mathcal{A}_k(t) + \mathcal{B}_k(t), \quad 0 \leq t \leq T, \quad (2.6)$$

where

$$\mathcal{A}_k(t) := 1 - \int_0^t \frac{1}{\mu(\tau)} d\tau - \int_0^t \int_0^\tau R_k(\tau, s) \frac{1}{\mu(s)} ds d\tau, \quad (2.7)$$

$$\mathcal{B}_k(t) := \int_0^t \frac{f_k(\tau)}{\mu(\tau)\lambda_k} d\tau + \int_0^t \int_0^\tau R_k(\tau, s) \frac{f_k(s)}{\mu(s)\lambda_k} ds d\tau. \quad (2.8)$$

Evaluating (2.6) at $t = T$ and using $u_k(T) = \psi_k$ gives

$$\psi_k = u_{0,k} \mathcal{A}_k(T) + \mathcal{B}_k(T).$$

By Lemma 2.3, $\mathcal{A}_k(T) > 0$ for all k , hence

$$u_{0,k} = \frac{\psi_k - \mathcal{B}_k(T)}{\mathcal{A}_k(T)}.$$

Substituting this into (2.6) yields

$$u_k(t) = \frac{\mathcal{A}_k(t)}{\mathcal{A}_k(T)} \psi_k + \mathcal{B}_k(t) - \frac{\mathcal{A}_k(t)}{\mathcal{A}_k(T)} \mathcal{B}_k(T).$$

Therefore, inserting into $u(x, t) = \sum_{k=1}^{\infty} u_k(t)e_k(x)$ and $u_0(x) = \sum_{k=1}^{\infty} u_{0,k}e_k(x)$ gives (2.1)–(2.2).

Convergence and regularity. We justify that the series representations define a classical solution in the sense of Definition 2.1. The argument is based on coefficient decay obtained by integration by parts, together with Bessel's inequality (2.3) and the Weierstrass M-test.

(a) *Preparatory coefficient estimates.* Under F2, integrating by parts twice in the definition of ψ_k gives

$$\psi_k = -\left(\frac{l}{\pi k}\right)^2 (\psi'')_k, \quad (\psi'')_k := \frac{2}{l} \int_0^l \psi''(x) \sin\left(\frac{k\pi}{l}x\right) dx, \quad (2.9)$$

and integrating once more yields

$$\psi_k = -\left(\frac{l}{\pi k}\right)^3 (\psi''')_k^c, \quad (\psi''')_k^c := \frac{2}{l} \int_0^l \psi'''(x) \cos\left(\frac{k\pi}{l}x\right) dx. \quad (2.10)$$

Therefore, by Cauchy–Schwarz and Bessel's inequality (2.3),

$$\sum_{k=1}^{\infty} |\psi_k| \leq \frac{l^2}{\pi^2} \sum_{k=1}^{\infty} \frac{1}{k^2} |(\psi'')_k| \leq \frac{l^2}{\pi^2} \left(\sum_{k=1}^{\infty} \frac{1}{k^4}\right)^{1/2} \left(\sum_{k=1}^{\infty} |(\psi'')_k|^2\right)^{1/2} \leq C \|\psi''\|_{L^2(0,l)}, \quad (2.11)$$

$$\sum_{k=1}^{\infty} \lambda_k |\psi_k| = \left(\frac{\pi}{l}\right)^2 \sum_{k=1}^{\infty} k^2 |\psi_k| \leq C \sum_{k=1}^{\infty} \frac{1}{k} |(\psi''')_k^c| \leq C \left(\sum_{k=1}^{\infty} \frac{1}{k^2}\right)^{1/2} \left(\sum_{k=1}^{\infty} |(\psi''')_k^c|^2\right)^{1/2} \leq C \|\psi'''\|_{L^2(0,l)}. \quad (2.12)$$

Similarly, under **F3**, integrating by parts twice in the definition of $f_k(t)$ gives, for a.e. $t \in (0, T)$,

$$f_k(t) = -\left(\frac{l}{\pi k}\right)^2 (f_{xx}(\cdot, t))_k, \quad (f_{xx}(\cdot, t))_k := \frac{2}{l} \int_0^l f_{xx}(x, t) \sin\left(\frac{k\pi}{l}x\right) dx. \quad (2.13)$$

Hence, for a.e. t ,

$$\sum_{k=1}^{\infty} |f_k(t)| \leq C \sum_{k=1}^{\infty} \frac{1}{k^2} |(f_{xx}(\cdot, t))_k| \leq C \|f_{xx}(\cdot, t)\|_{L^2(0,l)}, \quad (2.14)$$

and by Fubini and Cauchy–Schwarz in time,

$$\sum_{k=1}^{\infty} \int_0^T |f_k(t)| dt \leq C \int_0^T \|f_{xx}(\cdot, t)\|_{L^2(0,l)} dt \leq C\sqrt{T} \|f_{xx}\|_{L^2(0,T;L^2(0,l))} < \infty. \quad (2.15)$$

Moreover, if **F4** holds, then for every $\delta \in (0, T)$ we have

$$\sup_{t \in [\delta, T]} \sum_{k=1}^{\infty} |f_k(t)| \leq C \sup_{t \in [\delta, T]} \|f_{xx}(\cdot, t)\|_{L^2(0,l)} < \infty. \quad (2.16)$$

(b) *Uniform convergence of the series for u .* From the explicit mode representation

$$u_k(t) = \frac{\mathcal{A}_k(t)}{\mathcal{A}_k(T)} \psi_k + \mathcal{B}_k(t) - \frac{\mathcal{A}_k(t)}{\mathcal{A}_k(T)} \mathcal{B}_k(T),$$

and Lemma 2.3 (which yields $\mathcal{A}_k(T) > 0$), we obtain a k -uniform bound as follows. The Volterra resolvent construction and **F1** imply that there exists $C > 0$, independent of k , such that

$$\sup_{t \in [0, T]} |\mathcal{A}_k(t)| \leq C, \quad \sup_{t \in [0, T]} |\mathcal{B}_k(t)| \leq \frac{C}{\lambda_k} \int_0^T |f_k(s)| ds. \quad (2.17)$$

Consequently,

$$\sup_{t \in [0, T]} |u_k(t)| \leq C \left(|\psi_k| + \frac{1}{\lambda_k} \int_0^T |f_k(s)| ds \right) =: CM_k. \quad (2.18)$$

Since $|e_k(x)| \leq 1$ on $[0, l]$, it follows that

$$|u_k(t)e_k(x)| \leq CM_k, \quad (x, t) \in [0, l] \times [0, T].$$

Using (2.11), (2.15), and $\sum_{k \geq 1} \lambda_k^{-1} < \infty$, we get

$$\sum_{k=1}^{\infty} M_k \leq \sum_{k=1}^{\infty} |\psi_k| + \sum_{k=1}^{\infty} \frac{1}{\lambda_k} \int_0^T |f_k(s)| ds < \infty.$$

Therefore, by the Weierstrass M-test, the series (2.1) converges uniformly on $[0, l] \times [0, T]$. In particular, $u \in C([0, T]; C([0, l]))$.

(c) *Uniform convergence of the series for u_{xx} .* Differentiating formally in x gives

$$u_{xx}(x, t) = - \sum_{k=1}^{\infty} \lambda_k u_k(t) e_k(x).$$

We justify uniform convergence by estimating the k -th term: from (2.18),

$$\sup_{t \in [0, T]} \lambda_k |u_k(t)| \leq C \left(\lambda_k |\psi_k| + \int_0^T |f_k(s)| ds \right). \quad (2.19)$$

The right-hand side is summable in k by (2.12) and (2.15). Hence

$$\sum_{k=1}^{\infty} \sup_{t \in [0, T]} \lambda_k |u_k(t)| < \infty,$$

and since $|e_k(x)| \leq 1$, the Weierstrass M-test yields uniform convergence of the series for u_{xx} on $[0, l] \times [0, T]$. Thus $u_{xx} \in C((0, T) \times [0, l])$.

Moreover, by Cauchy–Schwarz and (2.13), for a.e. $t \in (0, T)$,

$$|f_k(t)| \leq C \frac{1}{k^2} \|f_{xx}(\cdot, t)\|_{L^2(0, l)}. \quad (2.20)$$

Indeed, by Cauchy–Schwarz and $|(f_{xx}(\cdot, t))_k| \leq C \|f_{xx}(\cdot, t)\|_{L^2(0, l)}$ (Bessel), the claim follows from (2.13). Consequently, if **F4** holds then for every $\delta \in (0, T)$,

$$\sup_{t \in [\delta, T]} |f_k(t)| \leq C \frac{1}{k^2} \sup_{t \in [\delta, T]} \|f_{xx}(\cdot, t)\|_{L^2(0, l)}. \quad (2.21)$$

In particular, $\sum_{k \geq 1} \sup_{t \in [\delta, T]} |f_k(t)| < \infty$.

(d) *Uniform convergence of the series for u_{xxt} on $[0, l] \times [\delta, T]$.* Assume **F4** and fix $\delta \in (0, T)$. Let $y_k(t) = u'_k(t)$. From the resolvent identity,

$$y_k(t) = g_k(t) + \int_0^t R_k(t, s) g_k(s) ds, \quad g_k(t) = \frac{f_k(t) - \lambda_k u_{0, k}}{\mu(t) \lambda_k}.$$

Standard resolvent (solution-operator) estimates for second-kind Volterra equations with weakly singular kernels imply that for every $\delta \in (0, T)$,

$$\sup_{t \in [\delta, T]} |y_k(t)| \leq C_\delta \|g_k\|_{L^\infty(\delta, T)}, \quad (2.22)$$

where C_δ depends only on (δ, T, α) and bounds on μ , but not on k ; see, e.g., Becker [36] (resolvent theory for weakly singular kernels). The k -independence follows since $\mu(t) \geq \mu_0$ and $1/\lambda_k \leq 1/\lambda_1$, so the kernel bounds entering the resolvent estimate are uniform in k .

Multiplying by λ_k and using $\mu(t) \geq \mu_0$ gives

$$\sup_{t \in [\delta, T]} \lambda_k |u'_k(t)| \leq C_\delta \left(\sup_{t \in [\delta, T]} |f_k(t)| + \lambda_k |u_{0, k}| \right). \quad (2.23)$$

Using $u_{0, k} = (\psi_k - \mathcal{B}_k(T))/\mathcal{A}_k(T)$ together with (2.17) yields

$$\lambda_k |u_{0, k}| \leq C \left(\lambda_k |\psi_k| + \int_0^T |f_k(s)| ds \right). \quad (2.24)$$

Combining (2.23)–(2.24) we arrive at

$$\sup_{t \in [\delta, T]} \lambda_k |u'_k(t)| \leq C_\delta \left(\sup_{t \in [\delta, T]} |f_k(t)| + \lambda_k |\psi_k| + \int_0^T |f_k(s)| ds \right). \quad (2.25)$$

We now show that the right-hand side is summable in k . By (2.21) we have $\sum_{k \geq 1} \sup_{t \in [\delta, T]} |f_k(t)| < \infty$. Moreover, $\sum_{k \geq 1} \lambda_k |\psi_k| < \infty$ by (2.12) and $\sum_{k \geq 1} \int_0^T |f_k(s)| ds < \infty$ by (2.15). Therefore,

$$\sum_{k=1}^{\infty} \sup_{t \in [\delta, T]} \lambda_k |u'_k(t)| < \infty.$$

Since $|e_k(x)| \leq 1$, the Weierstrass M-test implies that the series

$$u_{xxt}(x, t) = - \sum_{k=1}^{\infty} \lambda_k u'_k(t) e_k(x)$$

converges uniformly on $[0, l] \times [\delta, T]$. Hence $u_{xxt} \in C([0, l] \times [\delta, T])$.

(e) *Uniform convergence of the series for u_t on $[0, l] \times [\delta, T]$.* Assume **F4** and fix $\delta \in (0, T)$. From (2.25),

$$\sup_{t \in [\delta, T]} |u'_k(t)| \leq \frac{1}{\lambda_k} \sup_{t \in [\delta, T]} \lambda_k |u'_k(t)| \leq \frac{C_\delta}{\lambda_k} \left(\sup_{t \in [\delta, T]} |f_k(t)| + \lambda_k |\psi_k| + \int_0^T |f_k(s)| ds \right),$$

hence

$$\sup_{t \in [\delta, T]} |u'_k(t)| \leq C_\delta \left(|\psi_k| + \frac{1}{\lambda_k} \int_0^T |f_k(s)| ds + \frac{1}{\lambda_k} \sup_{t \in [\delta, T]} |f_k(t)| \right). \quad (2.26)$$

We show that the right-hand side is summable in k . First, $\sum_{k \geq 1} |\psi_k| < \infty$ by (2.11), and

$$\sum_{k \geq 1} \frac{1}{\lambda_k} \int_0^T |f_k(s)| ds < \infty$$

by (2.15) together with $\sum_{k \geq 1} \lambda_k^{-1} < \infty$.

Finally, using (2.21) and $\lambda_k = (\pi k/l)^2$, we obtain

$$\frac{1}{\lambda_k} \sup_{t \in [\delta, T]} |f_k(t)| \leq C \frac{1}{k^2} \cdot \frac{1}{k^2} \sup_{t \in [\delta, T]} \|f_{xx}(\cdot, t)\|_{L^2(0, l)} = C \frac{1}{k^4} \sup_{t \in [\delta, T]} \|f_{xx}(\cdot, t)\|_{L^2(0, l)}.$$

Hence $\sum_{k \geq 1} \lambda_k^{-1} \sup_{t \in [\delta, T]} |f_k(t)| < \infty$ since $\sum k^{-4} < \infty$.

Therefore,

$$\sum_{k=1}^{\infty} \sup_{t \in [\delta, T]} |u'_k(t)| < \infty.$$

Since $|e_k(x)| \leq 1$, the Weierstrass M-test implies that the series

$$u_t(x, t) = \sum_{k=1}^{\infty} u'_k(t) e_k(x)$$

converges uniformly on $[0, l] \times [\delta, T]$. In particular, $u_t \in C([0, l] \times [\delta, T])$. Moreover, by part (d) the series for $u_{xxt} = - \sum_{k \geq 1} \lambda_k u'_k(t) e_k(x)$ converges uniformly on $[0, l] \times [\delta, T]$, so $u_t(\cdot, t) \in C^2([0, l])$ and $(u_t)_{xx} = u_{xxt}$ on $[\delta, T]$.

Since each $u_k(\cdot) e_k(\cdot)$ is C^1 in t on $[\delta, T]$ and $\sum_{k \geq 1} u_k(t) e_k(x)$ converges uniformly on $[0, l] \times [\delta, T]$ (by (b)), while $\sum_{k \geq 1} u'_k(t) e_k(x)$ converges uniformly on $[0, l] \times [\delta, T]$ (by this step), the standard theorem on termwise differentiation of uniformly convergent series on compact sets implies that $u \in C^1([0, l] \times [\delta, T])$ and

$$u_t(x, t) = \sum_{k=1}^{\infty} u'_k(t) e_k(x) \quad \text{on } [0, l] \times [\delta, T].$$

Moreover, by (d) we have $(u_t)_{xx} = u_{xxt}$ on $[0, l] \times [\delta, T]$, hence $u \in C^1([\delta, T]; C^2([0, l]))$ for every $\delta \in (0, T)$, i.e. $u \in C^1((0, T); C^2([0, l]))$.

(f) *Uniform convergence of the series for $\partial_t^\alpha u$ on $[0, l] \times [\delta, T]$.* Fix $\delta \in (0, T)$ and assume **F4**. By the mode equation (2.5), for $t \in (0, T)$,

$$\partial_t^\alpha u_k(t) = f_k(t) + \lambda_k u_k(t) + \mu(t) \lambda_k u_k'(t).$$

Hence, for $t \in [\delta, T]$,

$$\partial_t^\alpha u(x, t) = \sum_{k=1}^{\infty} \partial_t^\alpha u_k(t) e_k(x) = \sum_{k=1}^{\infty} \left(f_k(t) + \lambda_k u_k(t) + \mu(t) \lambda_k u_k'(t) \right) e_k(x). \quad (2.27)$$

We show uniform convergence of the right-hand side on $[0, l] \times [\delta, T]$ termwise. For the first series, by (2.21) we have $\sum_{k \geq 1} \sup_{t \in [\delta, T]} |f_k(t)| < \infty$, and since $|e_k(x)| \leq 1$, the M-test yields uniform convergence of $\sum_{k \geq 1} f_k(t) e_k(x)$ on $[0, l] \times [\delta, T]$.

The second series $\sum_{k \geq 1} \lambda_k u_k(t) e_k(x)$ equals $-u_{xx}(x, t)$ and is uniformly convergent on $[0, l] \times [0, T]$ by part (c). The third series $\sum_{k \geq 1} \mu(t) \lambda_k u_k'(t) e_k(x)$ is uniformly convergent on $[0, l] \times [\delta, T]$ by part (d) and boundedness of μ on $[\delta, T]$. Therefore, (2.27) converges uniformly on $[0, l] \times [\delta, T]$, and in particular $\partial_t^\alpha u \in C([0, l] \times [\delta, T])$. Since $\delta \in (0, T)$ is arbitrary, we conclude $\partial_t^\alpha u \in C((0, T) \times [0, l])$.

Collecting (b)–(f), we obtain the stated regularity and the pointwise validity of (1.1).

Uniqueness. Let $(u_1, u_{0,1})$ and $(u_2, u_{0,2})$ be two classical solutions for the same (f, ψ) . Set $u := u_1 - u_2$ and $\chi := u_{0,1} - u_{0,2}$. Then u satisfies the homogeneous fractional pseudo-parabolic problem

$$\partial_t^\alpha u - u_{xx} - \mu(t) u_{xxt} = 0, \quad (x, t) \in (0, l) \times (0, T), \quad (2.28)$$

with boundary conditions $u(0, t) = u(l, t) = 0$, final-time measurement $u(x, T) = 0$, and initial state $u(x, 0) = \chi(x)$.

Expand u in the sine basis:

$$u(x, t) = \sum_{k=1}^{\infty} u_k(t) e_k(x), \quad e_k(x) = \sin\left(\frac{k\pi}{l} x\right), \quad \lambda_k = \left(\frac{k\pi}{l}\right)^2.$$

Then each coefficient u_k solves (with $f_k \equiv 0$)

$$\partial_t^\alpha u_k(t) + \mu(t) \lambda_k u_k'(t) + \lambda_k u_k(t) = 0, \quad 0 < t < T, \quad u_k(T) = 0, \quad (2.29)$$

and $u_k(0) = \chi_k$ (the sine coefficient of χ).

Repeating the derivation of the mode representation (Volterra reduction + resolvent), but with $f_k \equiv 0$, yields

$$u_k(t) = \chi_k \mathcal{A}_k(t), \quad 0 \leq t \leq T, \quad (2.30)$$

where $\mathcal{A}_k(t)$ is exactly the same functional defined in (2.7). Evaluating (2.30) at $t = T$ and using $u_k(T) = 0$, we get

$$0 = u_k(T) = \chi_k \mathcal{A}_k(T).$$

By lemma 2.3 we have $\mathcal{A}_k(T) \neq 0$ for every k , hence $\chi_k = 0$ for all k . Therefore $u_k(t) \equiv 0$ for all k and all $t \in [0, T]$, so $u \equiv 0$ on $(0, l) \times (0, T)$. In particular, $\chi = u(\cdot, 0) \equiv 0$, i.e. $u_{0,1} \equiv u_{0,2}$. □

Lemma 2.3 (Positivity of \mathcal{A}_k). *Let \mathcal{A}_k be the function defined by (2.7). Equivalently, \mathcal{A}_k is the solution of the homogeneous mode problem*

$$\partial_t^\alpha \mathcal{A}_k(t) + \mu(t)\lambda_k \mathcal{A}'_k(t) + \lambda_k \mathcal{A}_k(t) = 0, \quad t \in (0, T], \quad \mathcal{A}_k(0) = 1, \quad (2.31)$$

where ∂_t^α is the Caputo derivative.

Then:

(i) $\mathcal{A}_k \in AC([0, T])$ and for every $\delta \in (0, T)$ one has $\mathcal{A}_k \in C^1([\delta, T])$ and $\partial_t^\alpha \mathcal{A}_k \in C([\delta, T])$. In particular, (2.31) holds pointwise on $[\delta, T]$ for every $\delta > 0$.

(ii) $\mathcal{A}_k(t) > 0$ for all $t \in [0, T]$. Hence $\mathcal{A}_k(T) > 0$ for every $k \geq 1$.

Proof. Set $y_k(t) := \mathcal{A}'_k(t)$ and note that for $t \in [0, T]$,

$$\mathcal{A}_k(t) = 1 + \int_0^t y_k(s) ds, \quad \partial_t^\alpha \mathcal{A}_k(t) = \frac{1}{\Gamma(1-\alpha)} \int_0^t (t-s)^{-\alpha} y_k(s) ds.$$

Substituting into (2.31) and dividing by $\mu(t)\lambda_k$ gives, for a.e. $t \in (0, T)$, the Volterra equation of the second kind

$$y_k(t) + \int_0^t H_k(t, s) y_k(s) ds = -\frac{1}{\mu(t)}, \quad (2.32)$$

with weakly singular kernel

$$H_k(t, s) = \frac{1}{\mu(t)} + \frac{1}{\mu(t)\lambda_k\Gamma(1-\alpha)}(t-s)^{-\alpha}, \quad 0 \leq s < t \leq T.$$

Since μ is continuous and bounded away from 0 and $(t-s)^{-\alpha}$ is weakly singular with $\alpha \in (0, 1)$, the equation (2.32) falls within the class of weakly singular linear Volterra equations for which existence/uniqueness and resolvent-kernel representations are available; see Becker [36]. Consequently, y_k admits a (locally) continuous representative on $(0, T]$, and in particular $y_k \in C([\delta, T])$ for every $\delta \in (0, T)$. Therefore $\mathcal{A}_k \in AC([0, T])$ and $\mathcal{A}_k \in C^1([\delta, T])$ for every $\delta > 0$. In particular, choosing any $\delta \in (0, T)$, all terms in (2.31) are continuous on $[\delta, T]$ and thus (2.31) holds pointwise there.

Let $v \in AC([0, T])$ and let $t_0 \in (0, T]$ be such that $v(t_0) = \min_{0 \leq s \leq t_0} v(s)$. For AC functions the Caputo derivative admits the identity

$$\partial_t^\alpha v(t_0) = \frac{1}{\Gamma(1-\alpha)} \left(\frac{v(t_0) - v(0)}{t_0^\alpha} + \alpha \int_0^{t_0} \frac{v(t_0) - v(s)}{(t_0 - s)^{\alpha+1}} ds \right).$$

Since $v(t_0) \leq v(s)$ on $[0, t_0]$, the integral term is ≤ 0 , hence

$$\partial_t^\alpha v(t_0) \leq \frac{v(t_0) - v(0)}{\Gamma(1-\alpha)t_0^\alpha}. \quad (2.33)$$

Assume, for contradiction, that \mathcal{A}_k vanishes somewhere on $(0, T]$ and define the first hitting time

$$t_* := \inf\{t \in (0, T] : \mathcal{A}_k(t) = 0\}.$$

Then $\mathcal{A}_k(t) > 0$ for $t \in [0, t_*)$ and $\mathcal{A}_k(t_*) = 0$. Thus t_* is a minimizer of \mathcal{A}_k on $[0, t_*]$ with minimum 0. Applying (2.33) to $v = \mathcal{A}_k$ at t_* yields

$$\partial_t^\alpha \mathcal{A}_k(t_*) \leq \frac{\mathcal{A}_k(t_*) - \mathcal{A}_k(0)}{\Gamma(1-\alpha)t_*^\alpha} = \frac{0 - 1}{\Gamma(1-\alpha)t_*^\alpha} < 0.$$

On the other hand, since $t_* > 0$, choose $\delta \in (0, t_*)$. By Step 1, $\mathcal{A}_k \in C^1([\delta, T])$, so $\mathcal{A}'_k(t_*)$ exists and (2.31) holds pointwise at $t = t_*$. Using $\mathcal{A}_k(t_*) = 0$ in (2.31) gives

$$\partial_t^\alpha \mathcal{A}_k(t_*) = -\mu(t_*)\lambda_k \mathcal{A}'_k(t_*). \quad (2.34)$$

Moreover, $\mathcal{A}_k(t) > 0$ for $t < t_*$ and $\mathcal{A}_k(t_*) = 0$ implies $\mathcal{A}'_k(t_*) \leq 0$ (otherwise, if $\mathcal{A}'_k(t_*) > 0$, then $\mathcal{A}_k(t) < 0$ for $t < t_*$ sufficiently close to t_* , contradicting the definition of t_*). Since $\mu(t_*) \geq \mu_0 > 0$ and $\lambda_k > 0$, the right-hand side of (2.34) is ≥ 0 , hence $\partial_t^\alpha \mathcal{A}_k(t_*) \geq 0$. This contradicts $\partial_t^\alpha \mathcal{A}_k(t_*) < 0$ above.

Therefore \mathcal{A}_k cannot hit zero on $(0, T]$. Since $\mathcal{A}_k(0) = 1$, we conclude $\mathcal{A}_k(t) > 0$ for all $t \in [0, T]$, in particular $\mathcal{A}_k(T) > 0$. \square

2.3. Continuous dependence on the data. In this subsection, we prove that, under assumptions **F1–F3**, the reconstruction of the initial state $u_0(x) = u(x, 0)$ from the final-time measurement $\psi(x) = u(x, T)$ continuously depends on the data.

Proposition 2.4 (Stability estimate for the reconstructed initial state). *Assume **F1–F3**. Let (u, u_0) be the solution of the problem (1.1)–(1.3) given by (2.1)–(2.2). Then there exists a constant $C > 0$ (depending only on α, T, μ_0, l and bounds on μ) such that*

$$\|u_0\|_{L^2(0,l)} \leq C \left(\|\psi\|_{L^2(0,l)} + \sqrt{T} \|f\|_{L^2(0,T;L^2(0,l))} \right). \quad (2.35)$$

Moreover, for two data sets (ψ_1, f_1) and (ψ_2, f_2) with corresponding reconstructions $u_{0,1}, u_{0,2}$, one has

$$\|u_{0,1} - u_{0,2}\|_{L^2(0,l)} \leq C \left(\|\psi_1 - \psi_2\|_{L^2(0,l)} + \sqrt{T} \|f_1 - f_2\|_{L^2(0,T;L^2(0,l))} \right). \quad (2.36)$$

Proof. Recall that

$$u_0(x) = \sum_{k=1}^{\infty} u_{0,k} e_k(x), \quad u_{0,k} = \frac{\psi_k - \mathcal{B}_k(T)}{\mathcal{A}_k(T)}, \quad \lambda_k = \left(\frac{k\pi}{l} \right)^2.$$

A uniform lower bound for $\mathcal{A}_k(T)$. For \mathcal{A}_k we have (Lemma 2.3) $\mathcal{A}_k(t) > 0$ on $[0, T]$ and $\mathcal{A}_k \in AC([0, T])$. From the Volterra reduction (2.32) with negative right-hand side and positive kernel, the solution $y_k = \mathcal{A}'_k$ is nonpositive a.e., hence \mathcal{A}_k is nonincreasing. Therefore, for $t \in (0, T)$,

$$\partial_t^\alpha \mathcal{A}_k(t) = \frac{1}{\Gamma(1-\alpha)} \int_0^t (t-s)^{-\alpha} \mathcal{A}'_k(s) ds \leq 0.$$

Using the mode equation (2.31),

$$\mu(t)\lambda_k \mathcal{A}'_k(t) + \lambda_k \mathcal{A}_k(t) = -\partial_t^\alpha \mathcal{A}_k(t) \geq 0,$$

hence $\mathcal{A}'_k(t) \geq -\mu(t)^{-1} \mathcal{A}_k(t)$ for a.e. $t \in (0, T)$. By Grönwall's inequality,

$$\mathcal{A}_k(T) \geq \exp\left(-\int_0^T \frac{1}{\mu(s)} ds\right) \geq e^{-T/\mu_0}. \quad (2.37)$$

In particular, $\sup_{k \geq 1} \mathcal{A}_k(T)^{-1} \leq e^{T/\mu_0}$.

A bound for $\mathcal{B}_k(T)$. From the uniform estimate (2.17) (evaluated at $t = T$) there exists a constant $C_* > 0$ (independent of k and of the data) such that

$$|\mathcal{B}_k(T)| \leq \frac{C_*}{\lambda_k} \int_0^T |f_k(s)| ds. \quad (2.38)$$

Estimate of the Fourier coefficients $u_{0,k}$. Combining (2.37)–(2.38) yields

$$|u_{0,k}| \leq \frac{1}{\mathcal{A}_k(T)} \left(|\psi_k| + |\mathcal{B}_k(T)| \right) \leq e^{T/\mu_0} \left(|\psi_k| + \frac{C^*}{\lambda_k} \int_0^T |f_k(s)| ds \right).$$

Using $(a+b)^2 \leq 2a^2 + 2b^2$ and Cauchy–Schwarz in time,

$$\left(\int_0^T |f_k(s)| ds \right)^2 \leq T \int_0^T |f_k(s)|^2 ds, \quad \frac{1}{\lambda_k^2} \leq \frac{1}{\lambda_1^2}.$$

By Parseval,

$$\|u_0\|_{L^2(0,l)}^2 = \frac{l}{2} \sum_{k \geq 1} |u_{0,k}|^2, \quad \|\psi\|_{L^2(0,l)}^2 = \frac{l}{2} \sum_{k \geq 1} |\psi_k|^2, \quad \|f\|_{L^2(0,T;L^2(0,l))}^2 = \frac{l}{2} \sum_{k \geq 1} \int_0^T |f_k(t)|^2 dt.$$

Hence,

$$\|u_0\|_{L^2(0,l)}^2 \leq C \left(\|\psi\|_{L^2(0,l)}^2 + T \|f\|_{L^2(0,T;L^2(0,l))}^2 \right),$$

which implies (2.35) (after taking square roots and adjusting C).

Finally, (2.36) follows by applying the same argument to the difference data $(\psi_1 - \psi_2, f_1 - f_2)$, since the reconstruction is linear in (ψ, f) . \square

3. DISCRETISATION OF THE DIRECT MODEL

In this section, we describe the finite-difference discretisation used in the implementation for the time-fractional pseudo-parabolic direct problem

$$\partial_t^\alpha u(x, t) - u_{xx}(x, t) - \mu(t) u_{xxt}(x, t) = f(x, t), \quad (x, t) \in (0, l) \times (0, T), \quad (3.1)$$

subject to the homogeneous Dirichlet boundary conditions $u(0, t) = u(l, t) = 0$. We assume that $\mu \in C([0, T])$ and f is given. The Caputo derivative is discretised by an $L1$ -type scheme on a graded temporal mesh, while the spatial derivatives are approximated by second-order central differences. The resulting method leads to a tridiagonal linear system at each time level[38].

Spatial discretisation Let $x_i = ih$ for $i = 0, \dots, N$, where $h = l/N$. For a grid vector $\mathbf{v} = (v_1, \dots, v_{N-1})^\top \in \mathbb{R}^{N-1}$ we enforce the boundary conditions by setting $v_0 = v_N = 0$ and define the standard second-order discrete Laplacian $L_h : \mathbb{R}^{N-1} \rightarrow \mathbb{R}^{N-1}$ by

$$(L_h \mathbf{v})_i = \frac{v_{i-1} - 2v_i + v_{i+1}}{h^2}, \quad i = 1, \dots, N-1. \quad (3.2)$$

The matrix representation of L_h is symmetric tridiagonal and $(-L_h)$ is symmetric positive definite on \mathbb{R}^{N-1} .

We denote the interior nodal vector of the numerical solution by

$$\mathbf{u}^k := (u_1^k, \dots, u_{N-1}^k)^\top, \quad u_i^k \approx u(x_i, t_k),$$

where $\{t_k\}_{k=0}^M$ is the temporal grid defined below.

Time discretisation: Caputo derivative (L1 scheme) Let $0 = t_0 < t_1 < \dots < t_M = T$ be a time grid. In the implementation, we allow graded meshes of the form $t_k = T(k/M)^r$ with $r \geq 1$ (uniform mesh corresponds to $r = 1$). Set $\tau_k := t_k - t_{k-1}$. For each $k \geq 1$, we approximate the Caputo derivative at t_k using the $L1$ scheme

$$\partial_t^\alpha u(x_i, t_k) \approx \frac{1}{\Gamma(1-\alpha)} \sum_{j=1}^k \int_{t_{j-1}}^{t_j} \frac{u_t(x_i, s)}{(t_k - s)^\alpha} ds \approx \sum_{j=1}^k w_{k,j} (u_i^j - u_i^{j-1}), \quad (3.3)$$

where the weights $w_{k,j}$ depend on the mesh. For a nonuniform grid they can be written as

$$w_{k,j} = \frac{1}{\Gamma(2-\alpha)} d_{k,j}, \quad d_{k,j} = \frac{(t_k - t_{j-1})^{1-\alpha} - (t_k - t_j)^{1-\alpha}}{t_j - t_{j-1}}, \quad 1 \leq j \leq k. \quad (3.4)$$

Fully discrete scheme Using $u_{xxt} = (u_{xx})_t$ and the discrete Laplacian L_h , we approximate at time t_k :

$$u_{xx}(x_i, t_k) \approx (L_h \mathbf{u}^k)_i, \quad u_{xxt}(x_i, t_k) \approx \frac{(L_h \mathbf{u}^k)_i - (L_h \mathbf{u}^{k-1})_i}{\tau_k}.$$

Let $\mu^k := \mu(t_k)$ and

$$\mathbf{f}^k := (f(x_1, t_k), \dots, f(x_{N-1}, t_k))^\top.$$

Combining (3.3)–(3.4) with the above spatial discretisations yields, for $k = 1, \dots, M$, the linear system

$$\left(\frac{d_{k,k}}{\Gamma(2-\alpha)} I - \left(1 + \frac{\mu^k}{\tau_k} \right) L_h \right) \mathbf{u}^k = \mathbf{r}^k + \mathbf{f}^k - \frac{\mu^k}{\tau_k} L_h \mathbf{u}^{k-1}, \quad (3.5)$$

where \mathbf{r}^k collects the history (memory) contributions of the $L1$ approximation,

$$\mathbf{r}^k = \frac{d_{k,1}}{\Gamma(2-\alpha)} \mathbf{u}^0 + \frac{1}{\Gamma(2-\alpha)} \sum_{j=1}^{k-1} (d_{k,j+1} - d_{k,j}) \mathbf{u}^j. \quad (3.6)$$

Here $d_{k,j}$ are defined in (3.4). The left-hand side matrix in (3.5) is tridiagonal because L_h is tridiagonal. Therefore, at each time step the system is solved efficiently by the Thomas algorithm.

Given an initial state $u_0(x) = u(x, 0)$, we set

$$\mathbf{u}_{0,h} := (u_0(x_1), \dots, u_0(x_{N-1}))^\top \in \mathbb{R}^{N-1}, \quad \mathbf{u}^0 = \mathbf{u}_{0,h}.$$

The direct solver (3.5)–(3.6) then produces the discrete trajectory $\{\mathbf{u}^k\}_{k=0}^M$ and, in particular, the terminal vector \mathbf{u}^M used in the inverse step.

3.1. Stability–convergence analysis. We study the stability-convergence of the fully discrete method defined in (3.5)–(3.6). The Caputo derivative is discretised using the graded-mesh $L1$ formula, with weights $d_{k,j}$ specified in (3.4). Throughout, we assume

$$\mu \in C^1([0, T]), \quad 0 \leq \mu(t) \leq \mu_{\max}, \quad \|\mu'\|_{L^\infty(0, T)} \leq L_\mu, \quad (3.7)$$

and we use the discrete inner product and norms introduced earlier (in particular, the discrete Green identity $(-L_h \mathbf{v}, \mathbf{v})_h = \|\nabla_h \mathbf{v}\|_h^2$).

3.1.1. Preliminary properties of the graded-mesh $L1$ operator. Define the graded-mesh $L1$ operator (componentwise) by

$$\delta_t^\alpha \mathbf{v}^k := \frac{1}{\Gamma(2-\alpha)} \sum_{j=1}^k d_{k,j} (\mathbf{v}^j - \mathbf{v}^{j-1}), \quad k \geq 1, \quad (3.8)$$

with $d_{k,j}$ as in (3.4). For any admissible mesh (in particular, for graded meshes), one has

$$d_{k,j} > 0, \quad d_{k,1} \geq d_{k,2} \geq \dots \geq d_{k,k} \quad \text{for each fixed } k. \quad (3.9)$$

Lemma 3.1 (Coercivity of the graded-mesh $L1$ operator). *Let $\{\mathbf{v}^k\}_{k \geq 0} \subset \mathbb{R}^{N-1}$. Then, for each $k \geq 1$,*

$$(\delta_t^\alpha \mathbf{v}^k, \mathbf{v}^k)_h \geq \frac{1}{2} \delta_t^\alpha (\|\mathbf{v}^k\|_h^2), \quad (3.10)$$

where $\delta_t^\alpha (\|\mathbf{v}^k\|_h^2)$ is defined by applying (3.8) to the scalar sequence $\|\mathbf{v}^k\|_h^2$.

Proof. Using $(\mathbf{a} - \mathbf{b}, \mathbf{a})_h = \frac{1}{2}(\|\mathbf{a}\|_h^2 - \|\mathbf{b}\|_h^2 + \|\mathbf{a} - \mathbf{b}\|_h^2)$ term-by-term in (3.8) yields

$$(\delta_t^\alpha \mathbf{v}^k, \mathbf{v}^k)_h = \frac{1}{2\Gamma(2-\alpha)} \sum_{j=1}^k d_{k,j} \left(\|\mathbf{v}^j\|_h^2 - \|\mathbf{v}^{j-1}\|_h^2 + \|\mathbf{v}^j - \mathbf{v}^{j-1}\|_h^2 \right).$$

Dropping the nonnegative sum of increments $\sum d_{k,j} \|\mathbf{v}^j - \mathbf{v}^{j-1}\|_h^2$ gives (3.10). \square

3.1.2. Solvability at each time level. Let $\tau_k = t_k - t_{k-1}$ and $\mu^k = \mu(t_k)$. The time-stepping system (3.5) can be written as

$$\mathbf{A}^k \mathbf{u}^k = \mathbf{b}^k, \quad \mathbf{A}^k = \frac{d_{k,k}}{\Gamma(2-\alpha)} I - \left(1 + \frac{\mu^k}{\tau_k}\right) L_h, \quad (3.11)$$

where \mathbf{b}^k contains the history term (3.6), the source \mathbf{f}^k , and the contribution $-(\mu^k/\tau_k)L_h \mathbf{u}^{k-1}$ (see (3.5)).

Lemma 3.2 (Unique solvability). *Assume $\mu^k \geq 0$. Then \mathbf{A}^k is symmetric positive definite on \mathbb{R}^{N-1} for every $k \geq 1$, and (3.11) has a unique solution.*

Proof. For any $\mathbf{v} \neq 0$,

$$(\mathbf{A}^k \mathbf{v}, \mathbf{v})_h = \frac{d_{k,k}}{\Gamma(2-\alpha)} \|\mathbf{v}\|_h^2 + \left(1 + \frac{\mu^k}{\tau_k}\right) \|\nabla_h \mathbf{v}\|_h^2 > 0,$$

since $d_{k,k} > 0$ and $-L_h$ is SPD. \square

3.1.3. Stability estimate on a graded mesh.

Theorem 3.3 (Unconditional stability). *Let (3.7) hold and let $\{\mathbf{u}^k\}_{k=0}^M$ be generated by (3.5)–(3.6). Then there exists $C > 0$, depending on T, α, μ_{\max} and L_μ (but independent of h and the mesh sizes τ_k), such that for all $m \leq M$,*

$$\max_{0 \leq k \leq m} \|\mathbf{u}^k\|_h^2 + \sum_{k=1}^m \tau_k \|\nabla_h \mathbf{u}^k\|_h^2 + \max_{0 \leq k \leq m} \mu^k \|\nabla_h \mathbf{u}^k\|_h^2 \leq C \left(\|\mathbf{u}^0\|_h^2 + \sum_{k=1}^m \tau_k \|\mathbf{f}^k\|_h^2 \right). \quad (3.12)$$

Proof. Take the discrete inner product of (3.5) with \mathbf{u}^k . Using Lemma 3.1 and the Green identity gives

$$\frac{1}{2} \delta_t^\alpha (\|\mathbf{u}^k\|_h^2) + \|\nabla_h \mathbf{u}^k\|_h^2 + \mu^k \left(\frac{\nabla_h \mathbf{u}^k - \nabla_h \mathbf{u}^{k-1}}{\tau_k}, \nabla_h \mathbf{u}^k \right)_h \leq (\mathbf{f}^k, \mathbf{u}^k)_h. \quad (3.13)$$

The pseudo-parabolic term is treated by the identity

$$\left(\frac{\mathbf{a} - \mathbf{b}}{\tau_k}, \mathbf{a} \right)_h = \frac{1}{2\tau_k} \left(\|\mathbf{a}\|_h^2 - \|\mathbf{b}\|_h^2 + \|\mathbf{a} - \mathbf{b}\|_h^2 \right),$$

applied with $\mathbf{a} = \nabla_h \mathbf{u}^k$, $\mathbf{b} = \nabla_h \mathbf{u}^{k-1}$, which yields

$$\mu^k \left(\frac{\nabla_h \mathbf{u}^k - \nabla_h \mathbf{u}^{k-1}}{\tau_k}, \nabla_h \mathbf{u}^k \right)_h \geq \frac{1}{2\tau_k} \left(\mu^k \|\nabla_h \mathbf{u}^k\|_h^2 - \mu^k \|\nabla_h \mathbf{u}^{k-1}\|_h^2 \right). \quad (3.14)$$

We rewrite the right-hand term with μ^{k-1} :

$$-\mu^k \|\nabla_h \mathbf{u}^{k-1}\|_h^2 = -\mu^{k-1} \|\nabla_h \mathbf{u}^{k-1}\|_h^2 - (\mu^k - \mu^{k-1}) \|\nabla_h \mathbf{u}^{k-1}\|_h^2.$$

Since $|\mu^k - \mu^{k-1}| \leq L_\mu \tau_k$, we get

$$\frac{1}{2\tau_k} (\mu^k - \mu^{k-1}) \|\nabla_h \mathbf{u}^{k-1}\|_h^2 \leq \frac{L_\mu}{2} \|\nabla_h \mathbf{u}^{k-1}\|_h^2. \quad (3.15)$$

Finally, use Cauchy–Schwarz and discrete Poincaré to estimate

$$(\mathbf{f}^k, \mathbf{u}^k)_h \leq \|\mathbf{f}^k\|_h \|\mathbf{u}^k\|_h \leq C_P \|\mathbf{f}^k\|_h \|\nabla_h \mathbf{u}^k\|_h \leq \frac{1}{2} \|\nabla_h \mathbf{u}^k\|_h^2 + \frac{C_P^2}{2} \|\mathbf{f}^k\|_h^2.$$

Insert these bounds into (3.13), sum from $k = 1$ to m , and absorb the term $\sum_{k=1}^m \tau_k (L_\mu/2) \|\nabla_h \mathbf{u}^{k-1}\|_h^2$ by a discrete Grönwall argument. This yields (3.12). \square

3.1.4. *Convergence.* In what follows, we establish an error bound for the fully discrete scheme (3.5)–(3.6) on the graded time mesh

$$t_k = T \left(\frac{k}{M} \right)^r, \quad k = 0, 1, \dots, M, \quad r \geq 1, \quad (3.16)$$

with $\tau_k := t_k - t_{k-1}$ and $\tau_{\max} := \max_{1 \leq k \leq M} \tau_k$. We only refer to the discrete operators introduced in Section 3.

Error decomposition. Let u be the exact solution of the continuous problem and define its grid sampling at the interior nodes by

$$\mathbf{U}^k := (u(x_1, t_k), \dots, u(x_{N-1}, t_k))^\top, \quad k = 0, \dots, M.$$

Let $\{\mathbf{u}^k\}_{k=0}^M$ be the numerical solution produced by (3.5)–(3.6), and set the nodal error

$$\mathbf{e}^k := \mathbf{U}^k - \mathbf{u}^k, \quad k = 0, \dots, M.$$

By construction $\mathbf{e}^0 = \mathbf{0}$.

Assumption (graded-mesh regularity). Let $0 < \alpha < 1$, assume (3.7) with $\mu \geq 0$, and let $u_0 \in H^2(0, l) \cap H_0^1(0, l)$. Assume that the exact solution u fulfills, for every $(x, t) \in [0, l] \times (0, T]$,

$$|\partial_x^j u(x, t)| \leq C \quad \text{for } j = 0, 1, 2, 3, 4, \quad |\partial_t^i u(x, t)| \leq C(1 + t^{\alpha-i}) \quad \text{for } i = 0, 1, 2. \quad (3.17)$$

These bounds account for the initial-layer behaviour $\partial_t u \sim t^{\alpha-1}$ and are typical in graded-mesh L1 error analyses; see [37].

Error equation. Subtracting the discrete scheme (3.5) (applied to \mathbf{u}^k) from the same scheme written for the sampled exact solution \mathbf{U}^k yields, for $k = 1, \dots, M$,

$$\delta_t^\alpha \mathbf{e}^k - L_h \mathbf{e}^k - \mu^k \frac{L_h \mathbf{e}^k - L_h \mathbf{e}^{k-1}}{\tau_k} = \boldsymbol{\rho}^k, \quad \mathbf{e}^0 = \mathbf{0}, \quad (3.18)$$

where δ_t^α is the graded-mesh L1 operator (3.8) and $\boldsymbol{\rho}^k$ collects the local consistency errors of the temporal and spatial approximations.

Truncation error bound. Under (3.17), the spatial central difference approximation is second-order, hence

$$\|u_{xx}(\cdot, t_k) - L_h \mathbf{U}^k\|_h \leq Ch^2 \quad \text{for all } k.$$

Moreover, the pseudo-parabolic contribution $u_{xxt} = (u_{xx})_t$ is discretised by a backward difference in time, which gives

$$\left\| (u_{xx})_t(\cdot, t_k) - \frac{L_h \mathbf{U}^k - L_h \mathbf{U}^{k-1}}{\tau_k} \right\|_h \leq C\tau_k, \quad k \geq 1.$$

Finally, the graded-mesh $L1$ approximation of the Caputo derivative satisfies (cf. [37])

$$\max_{1 \leq k \leq M} \|\partial_t^\alpha u(\cdot, t_k) - \delta_t^\alpha \mathbf{U}^k\|_h \leq C M^{-\min\{2-\alpha, r\alpha\}}. \quad (3.19)$$

Combining these estimates yields, for $k = 1, \dots, M$,

$$\|\boldsymbol{\rho}^k\|_h \leq C \left(h^2 + \tau_k + M^{-\min\{2-\alpha, r\alpha\}} \right). \quad (3.20)$$

Theorem 3.4 (Convergence on a graded mesh). *Assume (3.7), (3.16), and the regularity condition (3.17). Let \mathbf{u}^k be the numerical solution of (3.5)–(3.6) and $\mathbf{e}^k = \mathbf{U}^k - \mathbf{u}^k$. Consequently, there is $C > 0$ (independent of h and M) such that*

$$\max_{0 \leq k \leq M} \|\mathbf{e}^k\|_h + \left(\sum_{k=1}^M \tau_k \|\nabla_h \mathbf{e}^k\|_h^2 \right)^{1/2} \leq C \left(h^2 + \tau_{\max} + M^{-\min\{2-\alpha, r\alpha\}} \right). \quad (3.21)$$

In particular, if $r \geq (2 - \alpha)/\alpha$, then the graded-mesh $L1$ contribution attains the optimal rate $M^{-(2-\alpha)}$. Since $\tau_{\max} = O(M^{-1})$ for (3.16), the overall temporal accuracy in (3.21) is limited by the first-order discretisation of the pseudo-parabolic term.

Proof. Apply the stability estimate of Theorem 3.3 to the error equation (3.18) (with source $\boldsymbol{\rho}^k$ and $\mathbf{e}^0 = \mathbf{0}$). This yields

$$\max_{0 \leq k \leq M} \|\mathbf{e}^k\|_h^2 + \sum_{k=1}^M \tau_k \|\nabla_h \mathbf{e}^k\|_h^2 \leq C \sum_{k=1}^M \tau_k \|\boldsymbol{\rho}^k\|_h^2.$$

Using (3.20) and the bounds $\sum_{k=1}^M \tau_k \leq T$ and $\sum_{k=1}^M \tau_k \tau_k^2 \leq T \tau_{\max}^2$, we obtain

$$\sum_{k=1}^M \tau_k \|\boldsymbol{\rho}^k\|_h^2 \leq C \left(h^4 + \tau_{\max}^2 + M^{-2\min\{2-\alpha, r\alpha\}} \right),$$

and taking square roots gives (3.21). \square

4. NUMERICAL RECONSTRUCTION OF THE INITIAL STATE

This section describes the fully discrete procedure used in our implementation to recover the unknown initial state $u_0(x) = u(x, 0)$ from the final-time measurement $\psi(x) = u(x, T)$ for the time-fractional pseudo-parabolic model

$$\partial_t^\alpha u(x, t) - u_{xx}(x, t) - \mu(t) u_{xxt}(x, t) = f(x, t), \quad (x, t) \in (0, l) \times (0, T), \quad (4.1)$$

with homogeneous Dirichlet boundary conditions. The method follows an ‘‘operator construction + Tikhonov’’ paradigm, where the forward map is generated by repeated runs of the fractional time-stepping solver.

4.1. Discrete inverse relation and forward map. Let $x_i = ih$, $i = 0, \dots, N$, with $h = l/N$, and let t_k be the time grid used by the Caputo discretisation (e.g. uniform or graded, $k = 0, \dots, M$). We denote by $\mathbf{u}^k \in \mathbb{R}^{N-1}$ the vector of interior values

$$\mathbf{u}^k := (u(x_1, t_k), \dots, u(x_{N-1}, t_k))^\top, \quad \mathbf{u}^0 = \mathbf{u}_{\mathbf{0}, h}.$$

The final-time measurement is sampled at interior points,

$$\boldsymbol{\psi}_h := (\psi(x_1), \dots, \psi(x_{N-1}))^\top \in \mathbb{R}^{N-1},$$

and the boundary constraints are enforced by fixing $u_0^k = u_N^k = 0$ for all k .

Discrete forward solution map. Let $\mathcal{S}_h : \mathbb{R}^{N-1} \rightarrow \mathbb{R}^{N-1}$ denote the discrete solution operator induced by the fractional solver (Caputo scheme in time + central differences in space) applied to (4.1). For a given initial vector $\mathbf{u}_{\mathbf{0}, h}$ and source f , the solver returns the terminal interior vector

$$\mathcal{S}_h(\mathbf{u}_{\mathbf{0}, h}; f) = \mathbf{u}^M(\mathbf{u}_{\mathbf{0}, h}; f).$$

The discrete inverse problem is then to determine $\mathbf{u}_{\mathbf{0}, h}$ such that

$$\mathbf{u}^M(\mathbf{u}_{\mathbf{0}, h}; f) \approx \boldsymbol{\psi}_h. \quad (4.2)$$

Affine splitting of the terminal state. Since the fully discrete scheme is linear in u , the final-time vector admits the decomposition

$$\mathbf{u}^M(\mathbf{u}_{\mathbf{0}, h}; f) = \mathbf{u}^M(\mathbf{u}_{\mathbf{0}, h}; 0) + \mathbf{u}^M(\mathbf{0}; f). \quad (4.3)$$

Define the forced contribution

$$\mathbf{g}_h := \mathbf{u}^M(\mathbf{0}; f) \in \mathbb{R}^{N-1},$$

and introduce the homogeneous forward operator $\mathbf{F}_h \in \mathbb{R}^{(N-1) \times (N-1)}$ by

$$\mathbf{u}^M(\mathbf{u}_{\mathbf{0}, h}; 0) = \mathbf{F}_h \mathbf{u}_{\mathbf{0}, h}.$$

Then (4.2) becomes the linear system

$$\mathbf{F}_h \mathbf{u}_{\mathbf{0}, h} = \boldsymbol{\psi}_h - \mathbf{g}_h =: \mathbf{d}_h. \quad (4.4)$$

Construction of \mathbf{F}_h by impulse responses. Let $\{\mathbf{e}^{(m)}\}_{m=1}^{N-1}$ be the canonical basis of \mathbb{R}^{N-1} . For each m , we run the *homogeneous* fractional solver ($f \equiv 0$) with initial data $\mathbf{u}^0 = \mathbf{e}^{(m)}$ and record the final-time vector

$$\mathbf{k}^{(m)} := \mathbf{u}^M(\mathbf{e}^{(m)}; 0).$$

The columns of \mathbf{F}_h are then assembled as

$$\mathbf{F}_h := [\mathbf{k}^{(1)} \ \mathbf{k}^{(2)} \ \dots \ \mathbf{k}^{(N-1)}].$$

This explicit assembly requires $N - 1$ homogeneous forward solves and is practical for moderate N (as in our experiments). For larger spatial grids, a matrix-free regularisation approach can be used to avoid forming \mathbf{F}_h explicitly.

4.2. Tikhonov regularisation. The backward reconstruction (4.4) is severely ill-conditioned, hence regularisation is required. We employ zeroth-order Tikhonov regularisation [39] and compute a stable approximation as the minimiser of

$$\mathcal{J}_\lambda(\mathbf{u}_{0,h}) = \frac{1}{2} \|\mathbf{F}_h \mathbf{u}_{0,h} - \mathbf{d}_h\|_2^2 + \frac{\lambda}{2} \|\mathbf{u}_{0,h}\|_2^2, \quad \lambda > 0. \quad (4.5)$$

The unique minimiser $\mathbf{u}_{0,h}^\lambda$ satisfies the normal equations

$$(\mathbf{F}_h^\top \mathbf{F}_h + \lambda I) \mathbf{u}_{0,h}^\lambda = \mathbf{F}_h^\top \mathbf{d}_h. \quad (4.6)$$

In the implementation, (4.6) is solved directly using a dense linear solver; the matrix $\mathbf{F}_h^\top \mathbf{F}_h + \lambda I$ is symmetric positive definite for all $\lambda > 0$.

4.3. Reconstruction procedure. Algorithm 1 summarises the reconstruction method consistent with the time-fractional forward solver.

Algorithm 1 Tikhonov reconstruction using the time-fractional pseudo-parabolic forward solver

Require: Spatial grid size N ; time grid $\{t_k\}_{k=0}^M$; interior final-time data $\psi_h \in \mathbb{R}^{N-1}$; regularisation parameter $\lambda > 0$; coefficient $\mu(t)$ and source $f(x, t)$; fractional forward solver for (4.1).

Ensure: Reconstructed initial vector $\mathbf{u}_{0,h}^\lambda \in \mathbb{R}^{N-1}$.

- 1: **Forced terminal term:** solve (4.1) with $\mathbf{u}^0 = \mathbf{0}$; set $\mathbf{g}_h := \mathbf{u}^M(\mathbf{0}; f)$.
 - 2: **Assemble \mathbf{F}_h :**
 - 3: **for** $m = 1, \dots, N - 1$ **do**
 - 4: solve (4.1) with $f \equiv 0$ and $\mathbf{u}^0 = \mathbf{e}^{(m)}$;
 - 5: set $\mathbf{F}_h(:, m) := \mathbf{u}^M(\mathbf{e}^{(m)}; 0)$.
 - 6: **end for**
 - 7: **Form data vector:** $\mathbf{d}_h := \psi_h - \mathbf{g}_h$.
 - 8: **Tikhonov solve:** compute $\mathbf{u}_{0,h}^\lambda$ from (4.6).
 - 9: **Output:** $\mathbf{u}_{0,h}^\lambda$.
-

Consistency check and error metrics. To verify the reconstruction, we re-run the forward solver with initial data $\mathbf{u}_{0,h}^\lambda$ (and the given f) to obtain a computed final-time vector $\hat{\psi}_h = \mathbf{u}^M(\mathbf{u}_{0,h}^\lambda; f)$ and compare it with ψ_h . When a reference initial state is available, we report the discrete errors

$$\|\mathbf{u}_{0,h}^\lambda - \mathbf{u}_{0,h}\|_\infty = \max_{1 \leq j \leq N-1} |u_{0,j}^\lambda - u_{0,j}|, \quad \|\mathbf{u}_{0,h}^\lambda - \mathbf{u}_{0,h}\|_{2,h} = \left(h \sum_{j=1}^{N-1} |u_{0,j}^\lambda - u_{0,j}|^2 \right)^{1/2},$$

and we additionally compute a final-time state mismatch in the same norms.

5. NUMERICAL VALIDATION AND EXPERIMENTS

In this section, we present numerical experiments that demonstrate the practical behaviour of the proposed regularised reconstruction of the *initial state* $u_0(x) = u(x, 0)$ from the *final-time measurement* $\psi(x) = u(x, T)$. All computations employ the direct solver from Section 3 and the discrete inverse formulation from Section 4.

5.1. Test setting and implementation details. Let $0 < \alpha < 1$ and $(x, t) \in [0, l] \times [0, T]$. We consider the manufactured solution

$$\mu(t) = 1 + t, \quad u(x, t) = (1 + t^{\alpha+1}) \sin\left(\frac{\pi x}{l}\right),$$

together with the forcing term chosen so that u satisfies the time-fractional pseudo-parabolic model, namely

$$f(x, t) = \left[\Gamma(\alpha + 2)t + \left(\frac{\pi}{l}\right)^2 (1 + t^{\alpha+1}) + \mu(t) \left(\frac{\pi}{l}\right)^2 (\alpha + 1)t^\alpha \right] \sin\left(\frac{\pi x}{l}\right).$$

Accordingly, the final-time measurement and initial state are

$$\psi(x) = u(x, T) = (1 + T^{\alpha+1}) \sin\left(\frac{\pi x}{l}\right), \quad u_0(x) = u(x, 0) = \sin\left(\frac{\pi x}{l}\right).$$

The direct solver produces interior nodal vectors; hence, the final-time measurement used in the inverse step is $\boldsymbol{\psi}_h = (\psi(x_1), \dots, \psi(x_{N-1}))^\top$. If the measured profile does not exactly satisfy $u(0, t) = u(l, t) = 0$, we enforce consistency by using only the interior samples and imposing zero boundary values at all time levels.

5.2. Noise-free validation. We begin with a noise-free study to verify that the direct solver and the reconstruction procedure are mutually consistent. In this setting, the final-time measurement is sampled from the exact formula, i.e. $\psi_i = \psi(x_i)$, $i = 1, \dots, N - 1$.

We fix $T = 1$ and refine the space–time grids according to

$$(N, M) \in \{(50, 50), (100, 100), (200, 200), (400, 400)\}.$$

For each grid, the implementation proceeds as follows: (i) compute the forced terminal contribution $\mathbf{g}_h = \mathbf{u}^M(\mathbf{0}; f)$; (ii) construct the homogeneous forward matrix \mathbf{F}_h by impulse responses; (iii) form the right-hand side $\mathbf{d}_h = \boldsymbol{\psi}_h - \mathbf{g}_h$; and (iv) obtain the regularised reconstruction by solving a Tikhonov system. To avoid notational duplication with the previous sections, we denote the reconstructed vector by $\widehat{\mathbf{u}}_{\mathbf{0}h}$ and write the normal equations in the equivalent form

$$(\mathbf{F}_h^\top \mathbf{F}_h + \lambda I) \widehat{\mathbf{u}}_{\mathbf{0}h} = \mathbf{F}_h^\top \mathbf{d}_h. \quad (5.1)$$

In the noise-free tests, we set $\lambda = 10^{-10}$ (the L-curve criterion gives values in the same range).

The maximum-norm and discrete L^2 errors for u_0 and the corresponding final-time consistency errors for ψ are listed in Table 1. The decay of all error indicators under refinement confirms the expected convergence of the overall discrete pipeline.

Figure 1 shows representative reconstructions for several values of α on a fixed grid ($N = M = 50$). For each α , the left panel compares the exact initial state $u_0(x)$ with its regularised reconstruction $\widehat{u}_0(x)$, while the right panel compares the exact final-time measurement $\psi(x)$ with the final-time state $u(x, T; \widehat{u}_0)$ obtained by forward propagation of the reconstructed initial state. The close agreement in both panels confirms the consistency of the inversion procedure and the direct solver.

Figure 2 compares the surface plot of the exact solution $u(x, t)$ with the reconstructed numerical approximation obtained from the final-time measurement, over the full time interval, for several values of α . It also displays the corresponding absolute error surfaces. All simulations use a fixed grid with $N = M = 200$.

TABLE 1. Reconstruction errors: L^∞ and L^2 -norm errors with noise-free terminal data.

α	(N,M)	$E_{u_0,\infty}$	$E_{u_0,2}$	$E_{\psi,\infty}$	$E_{\psi,2}$
0.1	(50, 50)	5.477e-03	3.873e-03	1.906e-10	1.348e-10
	(100, 100)	2.545e-03	1.799e-03	1.923e-10	1.360e-10
	(200, 200)	1.224e-03	8.653e-04	1.931e-10	1.365e-10
	(400, 400)	5.997e-04	4.241e-04	1.937e-10	1.371e-10
0.3	(50, 50)	1.371e-02	9.693e-03	1.882e-10	1.331e-10
	(100, 100)	6.698e-03	4.736e-03	1.908e-10	1.349e-10
	(200, 200)	3.310e-03	2.340e-03	1.918e-10	1.357e-10
	(400, 400)	1.645e-03	1.163e-03	1.870e-10	1.323e-10
0.5	(50, 50)	2.138e-02	1.512e-02	1.861e-10	1.316e-10
	(100, 100)	1.055e-02	7.460e-03	1.890e-10	1.336e-10
	(200, 200)	5.239e-03	3.704e-03	1.886e-10	1.334e-10
	(400, 400)	2.610e-03	1.845e-03	2.028e-10	1.434e-10
0.7	(50, 50)	2.893e-02	2.046e-02	1.840e-10	1.301e-10
	(100, 100)	1.433e-02	1.013e-02	1.879e-10	1.328e-10
	(200, 200)	7.124e-03	5.038e-03	1.889e-10	1.336e-10
	(400, 400)	3.550e-03	2.510e-03	1.941e-10	1.370e-10
0.9	(50, 50)	3.695e-02	2.613e-02	1.821e-10	1.287e-10
	(100, 100)	1.835e-02	1.297e-02	1.864e-10	1.318e-10
	(200, 200)	9.133e-03	6.458e-03	1.891e-10	1.336e-10
	(400, 400)	4.552e-03	3.218e-03	1.910e-10	1.349e-10

5.3. Reconstruction from noisy final-time data. In practice, the final-time measurement $\psi(x)$ is corrupted by measurement noise. To assess robustness, we perturb the discrete final-time vector by additive Gaussian noise with a prescribed *relative* level.

Let $\psi_h \in \mathbb{R}^{N-1}$ be the clean interior measurement. For $\delta > 0$, we set

$$\psi_h^\delta = \psi_h + \sigma_\delta \boldsymbol{\xi}, \quad \boldsymbol{\xi} \sim \mathcal{N}(\mathbf{0}, I_{N-1}), \quad \sigma_\delta := \delta \frac{\|\psi_h\|_2}{\sqrt{N-1}}. \quad (5.2)$$

With this choice, $\|\psi_h^\delta - \psi_h\|_2 / \|\psi_h\|_2 \approx \delta$ in expectation.

Given ψ_h^δ , we form $\mathbf{d}_h^\delta = \psi_h^\delta - \mathbf{g}_h$ and compute the regularised estimate $\widehat{\mathbf{u}}_{\mathbf{0},h}^\delta$ from

$$(\mathbf{F}_h^\top \mathbf{F}_h + \lambda I) \widehat{\mathbf{u}}_{\mathbf{0},h}^\delta = \mathbf{F}_h^\top \mathbf{d}_h^\delta. \quad (5.3)$$

To evaluate performance, we report initial-state errors relative to the exact discrete initial vector $\mathbf{u}_{\mathbf{0},h,\text{ex}}$,

$$E_{u_0,\infty}^\delta := \|\widehat{\mathbf{u}}_{\mathbf{0},h}^\delta - \mathbf{u}_{\mathbf{0},h,\text{ex}}\|_\infty, \quad E_{u_0,2}^\delta := \|\widehat{\mathbf{u}}_{\mathbf{0},h}^\delta - \mathbf{u}_{\mathbf{0},h,\text{ex}}\|_{2,h},$$

and final-time agreement against the noisy measurement,

$$E_{\psi,\infty}^\delta := \|\mathbf{u}^M(\widehat{\mathbf{u}}_{\mathbf{0},h}^\delta) - \psi_h^\delta\|_\infty, \quad E_{\psi,2}^\delta := \|\mathbf{u}^M(\widehat{\mathbf{u}}_{\mathbf{0},h}^\delta) - \psi_h^\delta\|_{2,h},$$

where $\|\cdot\|_{2,h} = \sqrt{h} \|\cdot\|_2$. Representative results for $\delta \in \{1\%, 3\%, 5\%\}$ are displayed in Table 2 for a fixed grid. As expected for backward reconstruction, larger noise levels lead to larger deviations in the recovered initial state. Nevertheless, the

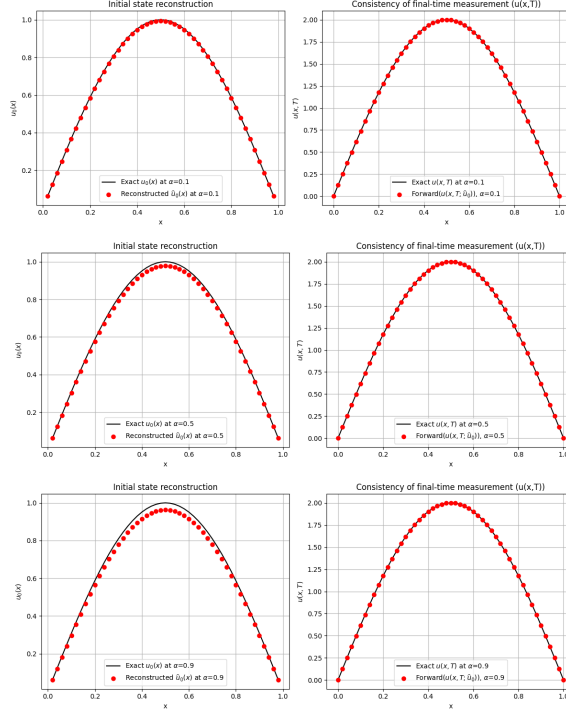


FIGURE 1. Reconstruction results for different fractional orders. Left: exact initial state $u_0(x)$ and reconstructed state $\widehat{u}_0(x)$. Right: exact final-time measurement $\psi(x)$ and the final-time state $u(x, T; \widehat{u}_0)$ generated by evolving the reconstructed initial state with the direct solver.

Tikhonov regularisation preserves the main shape of u_0 for moderate noise, and the corresponding forward solutions remain compatible with the perturbed final-time data, as illustrated in Figure 3.

Robustness with respect to noisy final-time data. Table 2 quantifies the sensitivity of the reconstruction to perturbations in the final-time measurement ψ . As expected for a backward (ill-posed) problem, the reconstruction error increases as the noise level δ grows. Nevertheless, the growth is controlled by the Tikhonov stabilisation: for $\delta = 1\%$ the recovered initial state remains accurate, with $E_{u_0,2}^\delta \approx (3.7\text{--}4.1) \times 10^{-2}$ and $E_{u_0,\infty}^\delta \approx (7.5\text{--}8.5) \times 10^{-2}$ across all tested fractional orders. When the noise is increased to $\delta = 3\%$ and $\delta = 5\%$, the initial-state errors rise in a near-proportional way (e.g., $E_{u_0,2}^\delta$ grows from $\approx 3.7 \times 10^{-2}$ to $\approx 1.1 \times 10^{-1}$ and then to $\approx 1.8 \times 10^{-1}$), indicating a stable dependence on the data perturbation rather than an uncontrolled blow-up.

A further observation is that the reported errors vary only mildly with α for fixed δ . This suggests that, for the present test, the regularised inversion is not overly sensitive to the fractional order, and the dominant factor affecting accuracy is the measurement noise level. In addition, the terminal-state mismatch $E_{\psi,\infty}^\delta$ and $E_{\psi,2}^\delta$ remains comparable to the noise magnitude, showing that the reconstructed initial

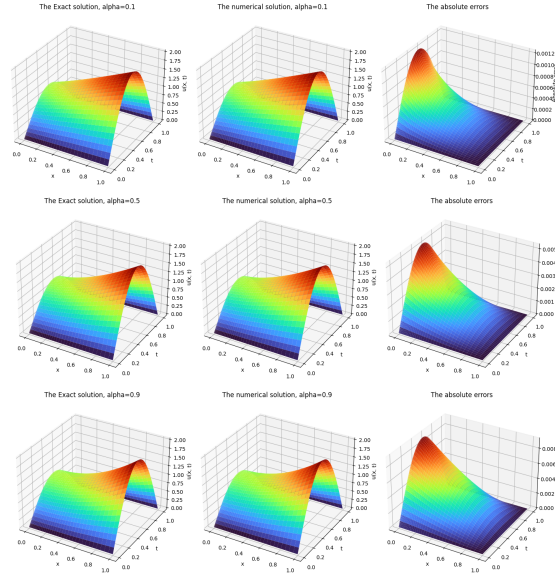


FIGURE 2. Exact solution (left), reconstructed solution (centre), and absolute error (right) for $u(x, t)$ for several values of α .

TABLE 2. Influence of additive noise in the final-time measurement ψ on the recovery of the initial state u_0 . Errors are reported for a fixed grid $N = M = 100$ and regularisation parameter $\lambda = 10^{-6}$.

α	noise level δ	$E_{u_0, \infty}^\delta$	$E_{u_0, 2}^\delta$	$E_{\psi, \infty}^\delta$	$E_{\psi, 2}^\delta$
0.1	1%	7.536e-02	3.655e-02	3.724e-02	1.828e-02
	3%	2.231e-01	1.090e-01	1.117e-01	5.483e-02
	5%	3.708e-01	1.815e-01	1.862e-01	9.138e-02
0.3	1%	7.776e-02	3.727e-02	3.724e-02	1.828e-02
	3%	2.255e-01	1.095e-01	1.117e-01	5.483e-02
	5%	3.732e-01	1.819e-01	1.862e-01	9.138e-02
0.5	1%	7.998e-02	3.818e-02	3.724e-02	1.828e-02
	3%	2.277e-01	1.100e-01	1.117e-01	5.483e-02
	5%	3.753e-01	1.823e-01	1.862e-01	9.138e-02
0.7	1%	8.226e-02	3.936e-02	3.724e-02	1.828e-02
	3%	2.299e-01	1.106e-01	1.117e-01	5.483e-02
	5%	3.776e-01	1.828e-01	1.828e-01	9.138e-02
0.9	1%	8.518e-02	4.120e-02	3.724e-02	1.828e-02
	3%	2.328e-01	1.115e-01	1.117e-01	5.483e-02
	5%	3.805e-01	1.835e-01	1.862e-01	9.138e-02

state produces forward solutions that stay consistent with the perturbed final-time measurement.

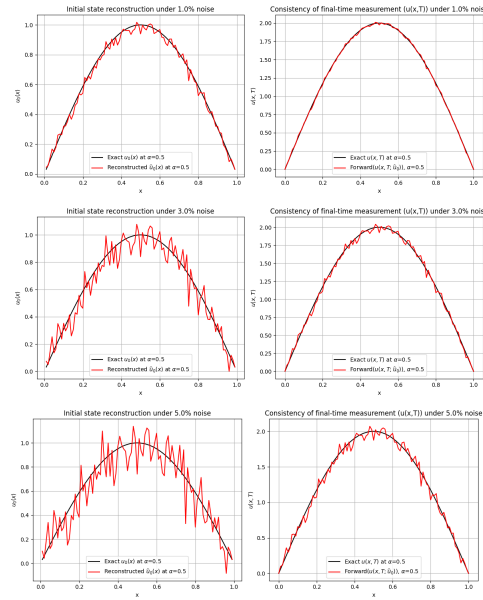


FIGURE 3. Recovered initial state $u_0^{\lambda, \delta}(x)$ for increasing noise levels δ in the final-time measurement, shown against the exact initial state $u_0(x)$.

Figure 4 shows surface plots of the reconstructed numerical result $u(x, t)$, obtained from the final-time measurement, for several noise levels over the full time interval with $\alpha = 0.5$.

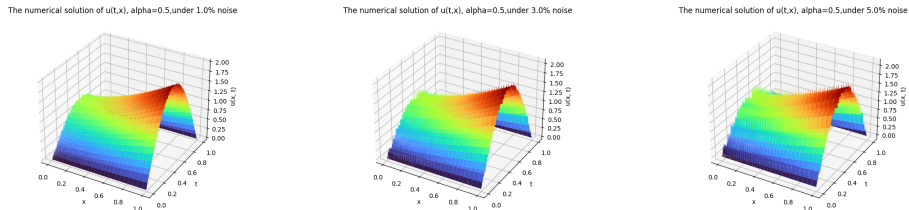


FIGURE 4. Numerical reconstructions of $u(x, t)$ over the full time interval using noisy data: 1% noise (left), 3% noise (middle), and 5% noise (right), for $\alpha = 0.5$.

Figures 3 and 4 complement these quantitative results: even for moderate noise, the reconstructed profiles preserve the main shape of the exact initial state, while higher noise levels primarily introduce smooth amplitude distortions rather than spurious oscillations. Overall, the experiments confirm that the proposed finite-difference-based forward solver combined with Tikhonov regularisation yields a numerically robust framework for recovering u_0 from noisy final-time data.

6. CONCLUSION

In this work, we have provided a comprehensive analysis of the backwards-in-time problem for a time-fractional pseudo-parabolic equation with time-dependent coefficients. From a theoretical standpoint, we established the existence and uniqueness of the problem. By employing a spectral expansion in terms of the eigenfunctions of the spatial operator and utilising the theory of Volterra integral equations, we proved the existence and uniqueness of the classical solution. We also derived stability estimates showing the continuous dependence of the initial data on the final-time measurements. Numerical treatments were developed for both the forward and inverse problems. For the direct problem, we constructed a fully discrete finite difference scheme using the $L1$ approximation on graded meshes for the Caputo derivative. We rigorously proved that the scheme is unconditionally stable and convergent, achieving an optimal convergence rate. Building upon this efficient forward solver, we formulated the inverse reconstruction as a minimisation problem regularised by the Tikhonov method. Numerical experiments confirmed the theoretical findings, demonstrating that the proposed algorithm effectively recovers the unknown initial state even in the presence of noise in the terminal data. Future research may extend this framework to multi-dimensional domains or non-linear source terms, where the interplay between memory effects and nonlinearity poses further challenges.

REFERENCES

- [1] G. I. Barenblatt, V. M. Entov, and V. M. Ryzhik. Theory of fluid flows through natural rocks. *Internat. J. Non-Linear Mech.*, 1989.
- [2] V. Padr'ón. Effect of aggregation on population recovery modeled by a forward-backward pseudo-parabolic equation. *Trans. Amer. Math. Soc.*, 356(7):2739–2756, 2004.
- [3] T. W. Ting. Certain non-steady flows of second-order fluids. *Arch. Rational Mech. Anal.*, 14:1–26, 1963.
- [4] T. B. Benjamin, J. L. Bona, and J. J. Mahony. Model equations for long waves in nonlinear dispersive systems. *Philos. Trans. Roy. Soc. London Ser. A*, 272(1220):47–78, 1972.
- [5] R. Huilgol. A second-order fluid of the differential type. *Internat. J. Non-Linear Mech.*, 3:471–482, 1968.
- [6] G. I. Barenblatt, I. Zheltov, and I. Kochina. Basic concepts in the theory of seepage of homogeneous liquids in fissured rocks. *J. Appl. Math. Mech.*, 24:1286–1303, 1960.
- [7] A. B. Al'shin, M. O. Korpusov, and A. G. Sveshnikov. Blow-up in nonlinear Sobolev-type equations, volume 15 of *De Gruyter Series in Nonlinear Analysis and Applications*. Walter de Gruyter & Co., Berlin, 2011.
- [8] V. G. Zvyagin and M. V. Turbin. Investigation of initial-boundary value problems for mathematical models of the motion of Kelvin-Voigt fluids. *Sovrem. Mat. Fundam. Napravl.*, 31:3–144, 2009.
- [9] Asanov, A., Atamanov, E.R.: *Nonclassical and Inverse Problems for Pseudoparabolic Equations*. De Gruyter, Berlin (1997)
- [10] Lorenzi, A., Paparoni, E.: Identification problems for pseudoparabolic integrodifferential operator equations. *J. Inv. Ill-Posed Probl.* 5, 235–253 (1997). <https://doi.org/10.1515/jiip.1997.5.3.235>
- [11] Fedorov, V.E., Urasaeva, A.V.: An inverse problem for linear Sobolev type equation. *J. Inverse Ill-posed Probl.* 12, 387–395 (2004). <https://doi.org/10.1515/1569394042248210>
- [12] Lyubanova, A.S., Tani, A.: An inverse problem for pseudoparabolic equation of filtration. The existence, uniqueness and regularity. *Appl. Anal.* 90, 1557–1568 (2011). <https://doi.org/10.1080/00036811.2010.530258>
- [13] Yaman, M.: Blow-up solution and stability to an inverse problem for a pseudo-parabolic equation. *J. Inequal. Appl.* 274, 1–8 (2012). <https://doi.org/10.1186/1029-242X-2012-274>

- [14] Bertsch M., Smarrazzo F., Tesei, A. Pseudo-parabolic regularization of forward-backward parabolic equations: Power-type nonlinearities. *Journal für die reine und angewandte Mathematik (Crelles Journal)*, vol. 2016, no. 712, 2016, pp. 51-80. <https://doi.org/10.1515/crelle-2013-0123>
- [15] Lyubanova, A.Sh., Velisevich, A.V.: Inverse problems for the stationary and pseudoparabolic equations of diffusion. *Appl. Anal.* 98, 1997–2010 (2019). <https://doi.org/10.1080/00036811.2018.1442001>
- [16] Antontsev, S.N., Aitzhanov, S.E., Ashurova, G.R.: An inverse problem for the pseudo-parabolic equation with p-Laplacian. *Evol. Equ. Control Theory* 11(2), 399–414 (2022). <https://doi.org/10.3934/eect.2021005>
- [17] Khompysh, K., Shakir, A.G.: An inverse source problem for a nonlinear pseudoparabolic equation with p-Laplacian diffusion and damping term. *Quaest. Math.* 46(9), 1889–1914 (2022). <https://doi.org/10.2989/16073606.2022.2115951>
- [18] Ruzhansky, M., Serikbaev, D., Torebek, B.T., Tokmagambetov, N.: Direct and inverse problems for time-fractional pseudo-parabolic equations. *Quaest. Math.* 45(7), 1071–1089 (2022)
- [19] Khompysh, K. Determination of a time-dependent source in semilinear pseudoparabolic equations with Caputo fractional derivative. *Chaos Solitons Fractals* 189, 115716 (2024) <https://doi.org/10.1016/j.chaos.2024.115716>
- [20] Khompysh, Kh., Huntul, M. J., Shazyndayeva, M. K., & Iqbal, M. K. (2024). An inverse problem for pseudoparabolic equation: existence, uniqueness, stability, and numerical analysis. *Quaestiones Mathematicae*, 47(10), 1979–2001. <https://doi.org/10.2989/16073606.2024.2347432>
- [21] B. Bekbolat, N. Tokmagambetov, *Inverse source problem for the pseudoparabolic equation associated with the Jacobi operator*, *Boundary Value Problems*. textbf52, 2024(1), (2024) <https://doi.org/10.1186/s13661-024-01859-x>
- [22] K. Van Bockstal and Kh. Khompysh. A time-dependent inverse source problem for a semilinear pseudo-parabolic equation with Neumann boundary condition. *Computers and Mathematics with Applications*, 208(2):97–112, 2026.
- [23] A. A. Kilbas, H. M. Srivastava, and J. J. Trujillo, *Theory and Applications of Fractional Differential Equations*, North-Holland: Mathematics studies, 2006.
- [24] Sakamoto, K.; Yamamoto, M. Initial value/boundary value problems for fractional diffusion-wave equations and applications to some inverse problems. *J. Math. Anal. Appl.* 2011, 382, 426–447.
- [25] 14 Wei, T.; Zhang, Y. The backward problem for a time-fractional diffusion-wave equation in a bounded domain. *Comput. Math. Appl.* 2018, 75, 3632–3648.
- [26] 10 Yang, F.; Zhang, Y.; Li, X. Landweber iterative method for identifying the initial value problem of the time-space fractional diffusion-wave equation. *Numer. Algorithms* 2020, 83, 1509–1530.
- [27] Floridia, G.; Li, Z.; Yamamoto, M. Well-posedness for the backward problems in time for general time-fractional diffusion equation. *Atti Accad. Naz. Lincei Rend. Lincei Mat. Appl.* 2020, 31, 593–610.
- [28] Floridia, G.; Yamamoto, M. Backward problems in time for fractional diffusion-wave equation. *Inverse Probl.* 2020, 36, 125016.
- [29] Luc N.H., Kumar D., Hang L.T.D, Can N.H. On a final value problem for a nonhomogeneous fractional pseudo-parabolic equation, *Alexandria Engineering Journal*, 59(6), 4353–4364 (2020).
- [30] 15 Zhang, Y.; Wei, T.; Zhang, Y.X. Simultaneous inversion of two initial values for a time-fractional diffusion-wave equation. *Numer. Methods Partial. Differ. Eqs.* 2021, 37, 24–43.
- [31] Long, L.D., Zhou, Y., Sakthivel, R. Tuan. N. H., Well-posedness and ill-posedness results for backward problem for fractional pseudo-parabolic equation. *J. Appl. Math. Comput.* 67, 175–206 (2021). <https://doi.org/10.1007/s12190-020-01488-4>
- [32] Yang, F., Xu, JM. & Li, X.X. Regularization methods for identifying the initial value of time fractional pseudo-parabolic equation. *Calcolo* 59, 47 (2022). <https://doi.org/10.1007/s10092-022-00492-3>
- [33] Yang, F., Xu, JM. & Li, X.X. Regularization methods for identifying the initial value of time fractional pseudo-parabolic equation. *Calcolo* 59, 47 (2022). <https://doi.org/10.1007/s10092-022-00492-3>

- [34] Di, H., Rong, W. The Regularized Solution Approximation of Forward/Backward Problems for a Fractional Pseudo-Parabolic Equation with Random Noise. *Acta Math Sci* 43, 324–348 (2023). <https://doi.org/10.1007/s10473-023-0118-3>
- [35] Serikbaev, D., Tokmagambetov, N. Determination of Initial Data in the Time-Fractional Pseudo-Hyperbolic Equation. *Symmetry* 2024, 16, 1332. <https://doi.org/10.3390/sym16101332>
- [36] Becker L. C., Resolvents and solutions of weakly singular linear Volterra integral equations, *Nonlinear Analysis: Theory, Methods & Applications*. – 2011. – Vol. 74, No. 5. – P. 1892–1912. <https://doi.org/10.1016/j.na.2010.10.060>
- [37] M. Stynes, E. O’Riordan, and J. L. Gracia, *Error analysis of a finite difference method on graded meshes for a time-fractional diffusion equation*, *SIAM J. Numer. Anal.* **55** (2017), 1057–1079. <https://doi.org/10.1137/16M1082329>
- [38] A. Altybay, *Numerical identification of a time-dependent coefficient in a time-fractional diffusion equation with integral constraints*, *Z. Angew. Math. Phys.* 77, 41 (2026). <https://doi.org/10.1007/s00033-025-02653-0>
- [39] Tikhonov, A.N., Arsenin, V.Y.: Solutions of ill-posed problems. *Math. Comput.* 32(144), 491–491 (1977)

ARSHYN ALTYBAY:

INSTITUTE OF MATHEMATICS AND MATHEMATICAL MODELING,
125 PUSHKIN STR., 050010 ALMATY, KAZAKHSTAN
INTERNATIONAL ENGINEERING AND TECHNOLOGICAL UNIVERSITY,
89/21 AL-FARABI AVENUE, ALMATY 050060, KAZAKHSTAN
AL-FARABI KAZAKH NATIONAL UNIVERSITY
71 AL-FARABI AVE., 050040 ALMATY, KAZAKHSTAN
DEPARTMENT OF MATHEMATICS: ANALYSIS, LOGIC AND DISCRETE MATHEMATICS,
GHENT UNIVERSITY, KRIJGSLAAN 281, BUILDING S8, B 9000 GHENT, BELGIUM
E-mail address arshyn.altybay@gmail.com